

Circular RNA profiling reveals circRNA1656 as a novel biomarker in high grade serous ovarian cancer

Yan Gao^{1,2}, Chuanqi Zhang¹, Yisi Liu¹, Min Wang^{1,*}

¹Department of Gynecology and Obstetrics, Shengjing Hospital Affiliated of China Medical University, Shenyang, Liaoning, China;

²Department of Gynecology, Cancer Hospital of China Medical University, Liaoning Cancer Hospital & Institute, Shenyang, Liaoning, China.

Summary

Circular RNA (circRNA) is a class of endogenous non-coding RNAs that are closely related to the pathogenesis of many human diseases, particularly cancer. However, the characterization of circRNAs in high-grade serous ovarian cancer (HGSOC) remains unknown. This study aimed to investigate the expression profile of circRNAs in HGSOC. Expression profiles of circRNAs differential expression based on circRNAs High-throughput sequencing were identified in 3 HGSOC specimens and 3 normal ovarian tissues. A total of 710 differentially expressed circRNAs were found (354 expressions up-regulated and 356 expressions down-regulated). CircRNA sequencing data were verified by qRT-PCR in HGSOC tissue and benign ovarian lesions. Differential expression of 7 circRNAs (circRNA385, circRNA2058, circRNA3336, circRNA2606, circRNA1656, circRNA1312 and circRNA7474) in HGSOC tissue was confirmed by qRT-PCR. Among them, circRNA1656 showed the highest fold change. qRT-PCR was used to verify the expression of circRNA1656 in ovarian cancer cell lines. In order to analyze the relationship between circRNA1656 expression and clinical pathological biological characteristics of HGSOC, qRT-PCR was used to verify the expression of circRNA1656 in 60 HGSOC tissues compared with 60 benign ovarian lesions. The expression of circRNA1656 was down-regulated in HGSOC tissues and ovarian cancer cell lines, and correlated with the FIGO stage of HGSOC. circRNA1656 has the potential to serve as a novel tumor marker for HGSOC.

Keywords: HGSOC, circular RNA, ovarian cancer, High-throughput sequencing, circular RNA profile, circRNA1656

1. Introduction

Ovarian cancer has the second highest incidence of gynecological malignant tumors, and is the leading cause of cancer-related mortality in the female reproductive system (1). The 5-year survival rate of Stage III-IV ovarian cancer is only 30% (2,3). Epithelial ovarian cancer (EOC) is the most important pathological subtype of ovarian cancer, accounting for more than 90%. Among the pathological subtypes of EOC, high-grade

ovarian serous carcinoma (HGSOC) accounts for 60-70% (4), the highest proportion. HGSOC often indicates a worse clinical outcome. Current studies have shown that HGSOC has a different pathogenesis from low-grade serous ovarian cancer. Despite the heterogeneity of HGSOC, the current treatment of clinical patients is not specific, further clarifying the pathogenesis of HGSOC and finding potential tumor markers or therapeutic targets are essential for improving the 5-year survival rate of HGSOC patients.

Circular RNAs (circRNAs) are characterized by a covalent closed-loop structure with no 5' cap or 3' polyadenylation tail (5,6), with the property of stable structure, good conservation, tissue specificity, and expression specificity at different developmental stages in different species (7). These unique features make circRNA a research hotspot.

To date, there is growing evidence that circRNAs

Released online in J-STAGE as advance publication April 24, 2019.

*Address correspondence to:

Dr. Min Wang, Department of Gynecology and Obstetrics, Shengjing Hospital Affiliated of China Medical University, No. 36 Sanhao Street, Heping District, Shenyang 110004, Liaoning, China.

E-mail: wm21st@126.com

are closely related to the pathogenesis of many human diseases, particularly cancer (8). So far, various types of cancer, including breast cancer (9), liver cancer (10), gastric cancer (11), colorectal cancer (12), and bladder cancer (13,14), have revealed abnormal expression levels of circRNA. However, ovarian cancer-based circRNAs research started late, with few studies. In a study by LINING *et al.* (15), circRNA sequencing analysis was performed in 4 matched EOCs and normal ovarian tissues. CircRNA sequencing data was verified by reverse transcription-quantitative polymerase chain reaction (qRT-PCR) in 54 EOC specimens and 54 normal ovarian tissues. In the subtype of EOC, existing studies have shown that HGSOC has a different pathogenesis from low-grade serous ovarian cancer. However, there has been no HGSOC-based circRNA study reported so far. So the aim of this study is to investigate the pathogenesis of HGSOC by high-throughput sequencing analysis of differential expression of circRNA in HGSOC specimens.

2. Materials and Methods

2.1. Clinical samples

A total of 120 cases were included. The postoperative pathology of all cases was confirmed by two chief physicians of the Department of Pathology of Liaoning Cancer Hospital & Institute, and all clinical data of the enrolled cases were collected. Among them, 60 cases of ovarian cancer cases were HGSOC; 60 cases in the control group were pathologically confirmed ovarian benign lesions. All cases had no history of tumors and radiochemotherapy. Among them, 3 cases of HGSOC and 3 cases of benign ovarian disease were chosen for High-throughput sequencing. The 6 selected cases were postmenopausal women with no endocrine diseases, metabolic diseases, infectious diseases and other medical history. This study was approved and supervised by The Ethics Committees of Liaoning Cancer Hospital & Institute, and written informed consent for participation was obtained from all subjects before sample collection.

2.2. Cell lines and culture

Ovarian cancer cells SKOV-3, HO 8910, and A2780 were purchased from Puno, Wuhan; OVCAR-3 was purchased from Zhongqiao Xinzhou, Shanghai; human ovarian epithelial cells were purchased from Saibai, Shanghai. All cells were cultured in a 37°C, 5% CO₂ incubator. SKOV3 was cultured in McCoy's 5A medium containing 10% fetal bovine serum; OVCAR-3 was cultured in RPMI-1640 medium containing 20% fetal bovine serum; A2780 was cultured in DMEM medium containing 10% fetal bovine serum; HO 8910, Human ovarian epithelial cells were cultured in RPMI-1640 medium containing 10% fetal bovine serum. The cells

used in the experiments were all in the logarithmic growth phase.

2.3. High-throughput sequencing

The experimental procedure was performed according to standard procedures provided by Illumina, including preparative libraries and sequencing experiments. Total RNA was treated with Trizol reagent (Invitrogen, CA, USA) according to the manufacturer's protocol. The purified RNA was randomly broken into short fragments by Fragmentation Buffer, and the fragmented circular RNA was used as a template to synthesize a strand of cDNA with six-base random primers (Random hexamers), followed by buffer and dNTPs. RNaseH and DNA Polymerase I for double-stranded cDNA synthesis. AMPure XP beads purified double-stranded product, using T4 DNA polymerase and klenow DNA polymerase activity to repair the sticky end of DNA to blunt end, 3' end plus base A and linker, AMPure XP beads for fragment selection, then USER enzyme. The second strand of cDNA containing U was degraded, and finally the final sequencing library was obtained by PCR amplification. After the library was qualified, it was sequenced by Illumina Hiseq 4000, and the sequencing read length was double-ended 2 × 150 bp (PE150).

The circRNA sequence itself was predicted by CIRC Explorer, the expression of these expressed circRNAs was quantified by the results of the tophat comparison, and dealt with the difference statistics between the circRNAs. The data results were statistically analyzed and graphically displayed using R language.

2.4. Quantitative real-time PCR (qRT-PCR)

RNA was extracted from cells and tissues. After RNA extraction, cDNA was synthesized by reverse transcription using super M-MLV reverse transcriptase (BioTeke, Beijing, China). The expression level of circRNA was evaluated by fluorescence quantitative analysis using an SYBR Green assay (Solarbio, Beijing, China) by an Exicycler™ 96 fluorescence meter (BIONEER, Korea). Primers designed to amplify circular transcripts are shown in Table 1. The relative levels of expression of selected circRNAs were measured using the 2^{-ΔΔCt} method.

2.5. GO and KEGG enrichment analysis

Functional analysis of differential genes included GO (Gene Ontology) enrichment analysis and KEGG (Kyoto Encyclopedia of Genes and Genomes) signal pathway enrichment analysis.

2.6. Statistical analysis

qRT-PCR validation is expressed as mean ± standard

Table 1. The primers for qRT-PCR

Name	Forward (from 5' to 3'),	Reverse(from 5' to 3'),
circRNA385	TGGGTCGGCCAGTCATGTAT	ACACAACTGCTTGCTCTACT
circRNA2606	ACCTCGATCTGTCCCAAGCA	GGTTTCTGCCCTGACACCTG
circRNA2058	TCAGGTGCTTTTCAGTGGGA	ACGCTTCAGCCTTTAAGACAGG
circRNA3336	AATGCTGCATTCCCCTCTCG	TCTCGAGACATGATGGCCCA
circRNA1656	CTGCGAGGTGGAGAAGGAGA	GACACACCCATGGCCATACG
circRNA2558	CGAAGTCGTTCAAGGGGTCG	AGAAGTCTCGAGGAGGACC
circRNA1312	GCTCAAGATCTTTGGCCAGAGC	GCATTGCCACTCCTCCAGAGA
circRNA7474	CCACAGCCTTGACAGTGTG3	TCAACACCAGAGTCGTGATCATGT
GAPDH	CAGGAGGCATTGCTGATGAT	GAAGGCTGGGGCTCATT

error of the mean. The comparison between HGSOC and benign ovarian lesions was performed by Student's *t* test (two-tailed). Chi-square test was used to analyze the correlation between circRNA1656 expression and clinical pathological biological characteristics. The *p* value < 0.05 was considered statistically significant.

3. Results and Discussion

3.1. CircRNA expression profile differentially expressed by HGSOC

12,291 different circRNA candidates were found in all samples. Then, we used *P* value < 0.05, with | log₂fold change | ≥ 1 to define the statistical criteria for selecting aberrantly expressed circRNA. A total of 710 circRNAs were differentially expressed, of which 354 were up-regulated and 356 were down-regulated. Including 693 exonics, 7 intronics, and 3 antisenses. Differential expression of circRNA between HGSOC group and benign ovarian lesion group was demonstrated by cluster analysis of heat map, volcano map and scatter plot.

According to the similarity of gene expression profiles of the samples, the genes were clustered and the differential gene clustering analysis heat map visually showed the expression of the genes in different samples. We used Log (FPKM+1) for gene expression display. Each column represents a sample, and each row represents a circRNA. The color scale reflects the log₂ signal strength, from green (low intensity) to black (medium intensity) to red (strong intensity). The hierarchical clustering map indicates the relative expression levels of circRNA in the HGSOC group and the normal ovarian group (Figure 1A).

The volcano map can be used to understand the overall distribution of differentially expressed circRNA. The volcano map was drawn for all genes in the differential expression analysis by using log₂ (fold change) as the abscissa and -log₁₀ (*p* value) as the ordinate. The abscissa represents the differential expression fold change of the gene in different samples; the ordinate represents the statistical significance of the difference in gene expression changes; the red dots represent significant differentially expressed transcripts, and the gray dots represent non-significant differentially

expressed transcripts (Figure 1B).

The circRNA differential expression scatter plot can visually display the differential expression of circRNA in HGSOC and benign ovarian lesions. Among them, the horizontal and vertical coordinates represent log₁₀ values of circRNA expression in tumor tissues and normal tissues, red represents differentially up-regulated circRNA, green represents differentially down-regulated circRNA, and blue represents non-differential circRNA (Figure 1C).

Studies have shown that circRNA plays an important role in the occurrence and development of tumors and has become a hot spot in cancer research. However, studies on the correlation between ovarian cancer and circRNA are rarely reported. Ahmed *et al.* (16) performed paired sequencing of the primary site, peritoneal and lymph node metastases in 3 patients with stage IIIC ovarian cancer, and analyzed the differential expression profiles of circRNA in the primary and metastatic sites of ovarian cancer. In the study of LINING *et al.* (15), circRNA sequencing analysis in 4 matched EOCs and normal ovarian tissues and qRT-PCR verification revealed that circEXOC6B and circN4BP2L2 are expected to be new markers of EOC. It is well known that EOC is rich in histopathological types, and the pathogenesis of HGSOC is different from that of low-grade serous ovarian cancer. Therefore, the circRNA expression profile of ovarian EOC differentially expressed by LINING *et al.* (15) has obvious limitations. Until now, the study of circRNA in HGSOC, the most common and poorly prognostic pathological subtype of ovarian cancer, has not been reported. This study analyzed the circRNA expression profile of HGSOC tissue for the first time, and found 354 up-regulated circRNAs, and 356 down-regulated CircRNAs.

3.2. GO and KEEG enrichment analysis of differentially expressed circRNAs

GO enrichment analysis is divided into three parts: biological process, molecular function and cell composition to interpret the function of differentially expressed circRNA. The results are shown in plot enriched GO DAG graph (Figure 2A) and histogram (Figure 2B). As shown, the top 5 rankings of biological

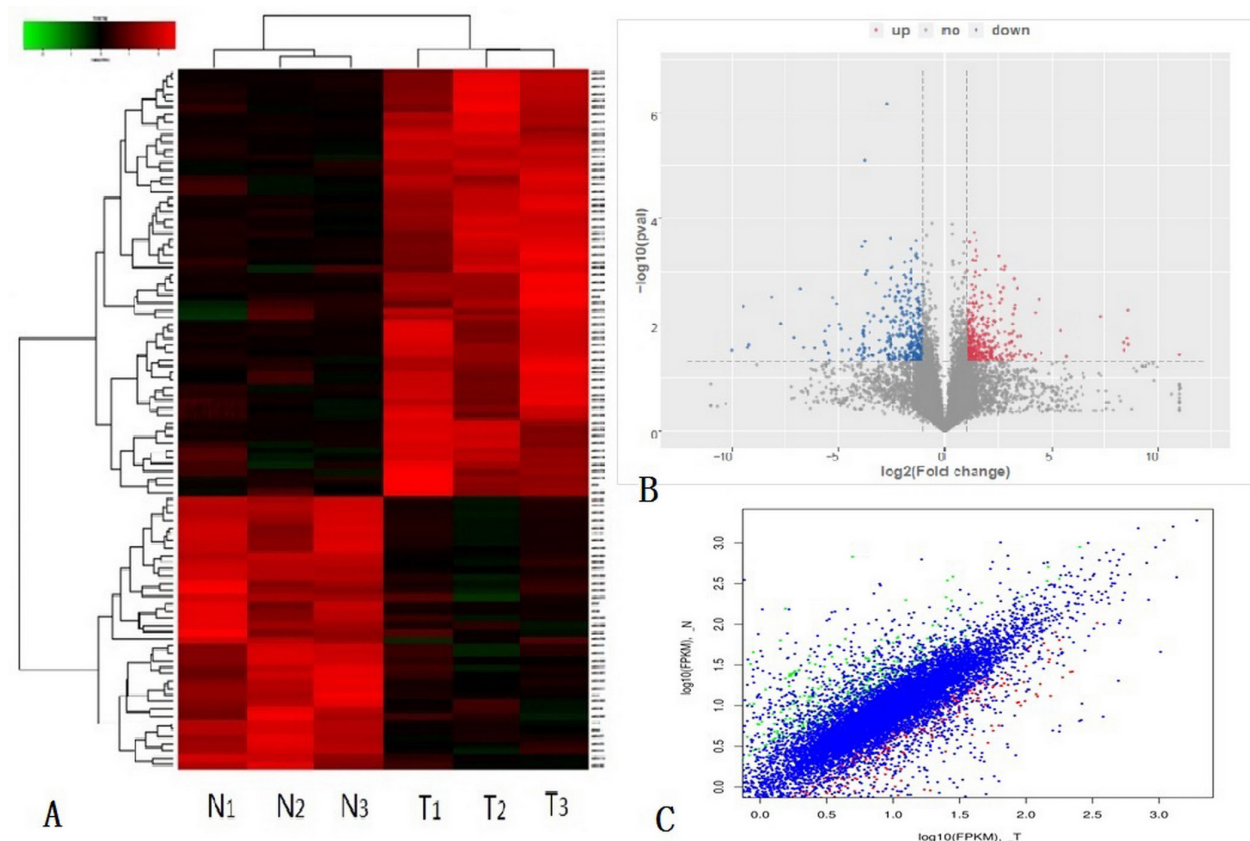


Figure 1. The differentially expressed circular RNAs (circRNAs). (A), Clustered heatmap. Each column represents a sample, and each row represents a circRNA. The color scale reflects the \log_2 signal strength, from green (low intensity) to black (medium intensity) to red (strong intensity). (B), Volcano plots. The red points in plot denote the differentially up-regulated expressed circRNAs with statistical significance while the green points denote down-regulated. (C), Scatter plot. Red represents differentially up-regulated circRNA, green represents differentially down-regulated circRNA, and blue represents non-differential circRNA.

processes in which differentially expressed circRNAs are predominantly involved in HGSOc are (1) regulation of transcription, DNA-templated, (2) transcription, DNA-templated, (3) signal transduction, (4) transport, (5) positive regulation of GTPase activity. The top 5 positions of the molecular functions of the differentially expressed circRNAs in HGSOc are (1) protein binding, (2) metal ion binding, (3) nucleotide binding, (4) DNA binding, and (5) ATP binding. The top 5 order of the cellular components involved in the differential expression of circRNA in HGSOc are (1) cytoplasm, (2) membrane, (3) nucleus, (4) cytosol, and (5) plasma membrane. The first cell component of the differentially expressed circRNAs in HGSOc was cytoplasm, and the vast majority of the differential expression in this study was exonic type, located in cytoplasm, consistent with the results of GO enrichment analysis.

KEEG enrichment analysis can present enrichment of possible pathways of action of differentially expressed circRNA in HGSOc. As shown, the pathways for differential expression of circRNA enrichment in HGSOc are (1) Pathways in cancer (2) Rap1 signaling pathway (3) PI3K-Akt signaling pathway (4) Tight junction (5) Proteoglycans in cancer (Figure 2C). Except for (4) tight junction, most pathways are closely related

to the pathogenesis of tumors. Rap1 plays a key role in the development and progression of cancer. It inhibits the transformation of oncogene Ras-induced cells; it also induces malignant transformation of cells by a switch molecule on the cell signaling pathway through interaction with its downstream target molecules (17). The PI3K-Akt signaling pathway is involved in the regulation of various cellular functions such as cell proliferation, differentiation, apoptosis, and glucose transport, and is associated with a variety of tumors (18).

3.3. qRT-PCR verification High-throughput sequencing results

Based on differential expression of circRNA fold change, p value, FDR and fpkm, we selected 8 circRNAs for qRT-PCR validation (Table 2). Validation was performed in 40 HGSOc tissues and 40 ovarian benign lesions.

The results showed that the fold change of circRNA2558 was down-regulated in qRT-PCR, which was inconsistent with circRNA-seq results (up-regulated) ($p < 0.05$). circRNA385, circRNA2058, circRNA3336, circRNA2606 and circRNA1656 expression were down-regulated and qRT-PCR results were consistent with circRNA-seq results ($p < 0.05$). The expression of

circRNA1312 and circRNA7474 were up-regulated, and the qRT-PCR results were consistent with the circRNA-seq results ($p < 0.05$). The results of qRT-PCR verified in the tissue were consistent with the circRNA-seq results, which further validated the reliability of our circRNA-

seq results (Figure 3).

CircRNA has tissue-specific and developmental stage specificity (19,20). The unique closed-loop structure makes circRNA insensitive to ribonuclease and is highly stable, allowing it to be fully expressed in various

Table 2. The 8 circRNAs chosen to validate High-throughput sequencing by qRT-PCR

CircRNA ID	Chrom	CircRNA Type	Gene symbol	Log2Fold change	P value
CircRNA385	Chr11	Exonic	HIPK3	-1.24	0.04
CircRNA2058	Chr5	Exonic	RHOBTB3	-3.85	0.01
CircRNA3336	Chr9	Exonic	BNC2	-2.30	0.00
CircRNA2606	Chr3	Exonic	LRCH3	-1.38	0.04
CircRNA2558	Chr3	Exonic	RSRC1	1.06	0.02
CircRNA1656	Chr7	Exonic	CLIP2	-1.09	0.03
CircRNA1312	Chr19	Exonic	ZNY208	2.26	0.01
CircRNA7474	Chr1	Exonic	STIL	2.53	0.00

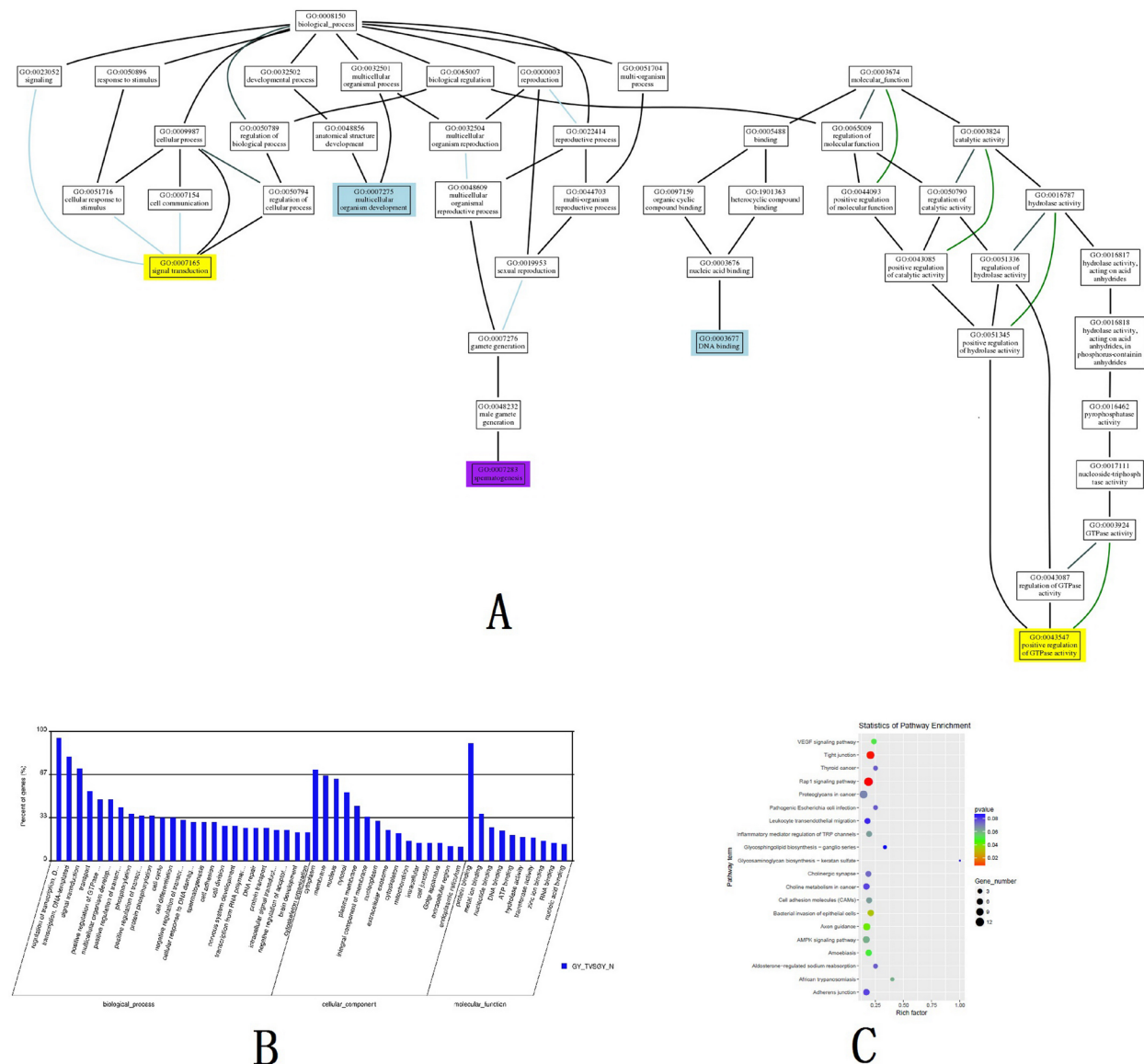


Figure 2. GO and KEEG enrichment analysis of differentially expressed circRNAs between HGSOC group and benign ovarian lesions group. (A), GO enrichment analysis showed by plot enriched GO DAG graph. **(B),** GO enrichment analysis is divided into three parts: biological process, molecular function and cell composition, a list of differential gene expression shows abundances number for the function. **(C),** Scatter plot of KEEG enrichment analysis. The vertical axis shows the annotated significantly enriched pathway of the significant differentially expressed gene. The horizontal axes shows the rich factor.

of proteins to cell membranes to play a biological role. GPI is the only way in which proteins bind to the cell membrane, and many receptors, antigens, and biologically active proteins have been shown to bind to cell membranes through GPI structures (27).

3.5. CircRNA-miRNA network map of circRNA1656

Current studies have shown that the competitive inhibition of molecular sponges as miRNAs is the most important mechanism of action of circRNA. To explore the possible mechanism of action of circRNA1656, based on bioinformatics and information mining, predict miRNAs that may interact with circRNA1656 and map circRNA-miRNA networks (Figure 4B).

3.6. Detection of circRNA1656 expression in ovarian cancer cell lines by qRT-PCR

qRT-PCR was used to detect the expression of circRNA1656 in human ovarian epithelial cells, ovarian cancer cells SKOV3, OVCAR-3, HO8910, and A2780 for the purpose of further verification of the circRNA-seq results. The expression of circRNA1656 ($2^{-\Delta\Delta Ct}$) in the ovarian cancer cells were compared with human ovarian epithelial cells (the average of $2^{-\Delta\Delta Ct}$ was 1.0). The results showed that circRNA1656 in the ovarian cancer cells were all significantly down-regulated. The p value was < 0.01 (Figure 4C). This result is consistent with the results of circRNA-seq.

3.7. Detection of circRNA1656 expression in HGSOc tissue by qRT-PCR

In order to further clarify the expression of circRNA1656 in HGSOc tissues, qRT-PCR was performed in 60 HGSOc tissues and 60 benign ovarian lesions. The results showed that the expression level and overall expression level of circRNA1656 in HGSOc tissues was lower than that in the ovarian benign lesion group, and the difference was statistically significant (Figure 4D and 4E).

3.8. Relationship between circRNA1656 expression and clinical pathological biological characteristics of HGSOc

In order to analyze the relationship between circRNA1656 expression and clinical pathological biological characteristics of HGSOc, 60 cases of HGSOc patients were divided into 2 groups (low expression group and high expression group) according to the the median of ΔCt expression of circRNA1656 (11.9). The results showed that the expression of circRNA1656 was correlated with the patient's FIGO stage ($p = 0.012$), and the difference was statistically significant. There was no correlation among

Table 3. Relationship between circRNA1656 expression and clinical pathological biological characteristics of HGSOc

clinical characteristics	cases (n = 60)	circRNA1656 expression		P value
		low	high	
menopause				0.475
yes	27	14	13	
no	33	18	15	
ascites				0.0641
yes	22	9	13	
no	38	23	15	
FIGO stage				0.012
I-II	15	4	11	
III-IV	45	28	17	
LN metastasis				0.392
Positive	36	19	17	
negative	24	13	11	
CA-125				0.285
Normal	12	6	6	
Increasing	48	26	22	

menopause, ascites, LN metastasis and CA-125 level with the expression of circRNA ($p > 0.05$) (Table 3).

In conclusion, this study is the high-throughput sequencing study of HGSOc to find differential expression profiles of circRNA for the first time. A total of 354 circRNA expressions were up-regulated and 356 circRNA expression was down-regulated. qRT-PCR confirmed circRNA385, circRNA2058, circRNA3336, circRNA2606, and circRNA1656 were all down-regulated in HGSOc tissues, while circRNA1312 and circRNA7474 were up-regulated in HGSOc tissues ($p < 0.05$), consistent with circRNA-seq results. circRNA1656 was down-regulated in both HGSOc tissue and ovarian cancer cell lines, and was significantly associated with HGSOc FIGO stage, and is expected to become a novel tumor marker for HGSOc.

Acknowledgements

This work was supported by Research Foundation of Science and Technology Bureau, Shenyang city (18-014-4-61). And this work was also supported by the Outstanding Scientific Fund of Shengjing Hospital (Grant No. 201705).

References

1. Torre LA, Bray F, Siegel RL, Ferlay J, Lortet-Tieulent J, Jemal A. Global cancer statistics, 2012. *CA Cancer J Clin.* 2015; 65:87-108.
2. Siegel RL, Miller KD, Jemal A. Cancer statistics, 2016. *CA Cancer J Clin.* 2016; 66:7-30.
3. Kim JH, Park CW, Um D, Baek KH, Jo Y, An H, Kim Y, Kim TJ. Mass spectrometric screening of ovarian cancer with serum glycans. *Dis Markers.* 2014; 2014:634289.
4. Bachmayr-Heyda A, Auer K, Sukhbaatar N, Aust S, Deycmar S, Reiner AT, Polterauer S, Dekan S, Pils

- D. Small RNAs and the competing endogenous RNA network in high grade serous ovarian cancer tumor spread. *Oncotarget*. 2016; 7:39640-39653.
5. Lasda E, Parker R. Circular RNAs: Diversity of form and function. *RNA*. 2014; 20:1829-1842.
 6. Cortes-Lopez M, Miura P. Emerging functions of circular RNAs. *Yale J Biol Med*. 2016; 89:527-537.
 7. Wang Y, Lu T, Wang Q, Liu J, Jiao W. Circular RNAs: Crucial regulators in the human body (Review). *Oncol Rep*. 2018; 40:3119-3135.
 8. Chen Y, Li C, Tan C, Liu X. Circular RNAs: A new frontier in the study of human diseases. *J Med Genet*. 2016; 53:359-365.
 9. Kristensen LS, Hansen TB, Venø MT, Kjems J. Circular RNAs in cancer: Opportunities and challenges in the field. *Oncogene*. 2018; 37:555-565.
 10. Qin M, Liu G, Huo X, Tao X, Sun X, Ge Z, Yang J, Fan J, Liu L, Qin W. Hsa_circ_0001649: A circular RNA and potential novel biomarker for hepatocellular carcinoma. *Cancer Biomark*. 2016; 16:161-169.
 11. Li P, Chen H, Chen S, Mo X, Li T, Xiao B, Yu R, Guo J. Circular RNA 0000096 affects cell growth and migration in gastric cancer. *Br J Cancer*. 2017; 116:626-633.
 12. Huang G, Zhu H, Shi Y, Wu W, Cai H, Chen X. *circ-ITCH* plays an inhibitory role in colorectal cancer by regulating the Wnt/beta-catenin pathway. *PLoS One*. 2015; 10:e0131225.
 13. Zhong Z, Lv M, Chen J. Screening differential circular RNA expression profiles reveals the regulatory role of circTCF25-miR-103a-3p/miR-107-CDK6 pathway in bladder carcinoma. *Sci Rep*. 2016; 6:30919.
 14. Yang X, Yuan W, Tao J, Li P, Yang C, Deng X, Zhang X, Tang J, Han J, Wang J, Li P, Lu Q, Gu M. Identification of circular RNA signature in bladder cancer. *J Cancer*. 2017; 8:3456-3463.
 15. Ning L, Long B, Zhang W, Yu M, Wang S, Cao D, Yang J, Shen K, Huang Y, Lang J. Circular RNA profiling reveals circEXOC6B and circN4BP2L2 as novel prognostic biomarkers in epithelial ovarian cancer. *Int J Oncol*. 2018; 53:2637-2646.
 16. Ahmed I, Karedath T, Andrews SS, Al-Azwani IK, Mohamoud YA, Querleu D, Rafii A, Malek JA. Altered expression pattern of circular RNAs in primary and metastatic sites of epithelial ovarian carcinoma. *Oncotarget*. 2016; 7:36366-36381.
 17. Chrzanowska-Wodnicka M. Rap1 in endothelial biology. *Curr Opin Hematol*. 2017; 24:248-255.
 18. Haddadi N, Lin Y, Travis G, Simpson AM, Nassif NT, McGowan EM. PTEN/PTENP1: 'Regulating the regulator of RTK-dependent PI3K/Akt signalling', new targets for cancer therapy. *Mol Cancer*. 2018; 17:37.
 19. Salzman J, Chen RE, Olsen MN, Wang PL, Brown PO. Cell-type specific features of circular RNA expression. *PLoS Genet*. 2013; 9:e1003777.
 20. Memczak S, Jens M, Elefsinioti A, *et al*. Circular RNAs are a large class of animal RNAs with regulatory potency. *Nature*. 2013; 495:333-338.
 21. Bahn JH, Zhang Q, Li F, Chan TM, Lin X, Kim Y, Wong DT, Xiao X. The landscape of microRNA, Piwi-interacting RNA, and circular RNA in human saliva. *Clinical chemistry*. 2015; 61:221-230.
 22. Vandeweyer G, Van der Aa N, Reyniers E, Kooy RF. The contribution of CLIP2 haploinsufficiency to the clinical manifestations of the Williams-Beuren syndrome. *Am J Hum Genet*. 2012; 90:1071-1078.
 23. Delgado LM, Gutierrez M, Augello B, Fusco C, Micale L, Merla G, Pastene EA. A 1.3-mb 7q11.23 atypical deletion identified in a cohort of patients with williams-beuren syndrome. *Mol Syndromol*. 2013; 4:143-147.
 24. Selmansberger M, Kaiser JC, Hess J, Guthlin D, Likhtarev I, Shpak V, Tronko M, Brenner A, Abend M, Blettner M, Unger K, Jacob P, Zitzelsberger H. Dose-dependent expression of CLIP2 in post-Chernobyl papillary thyroid carcinomas. *Carcinogenesis*. 2015; 36:748-756.
 25. Hess J, Thomas G, Braselmann H, Bauer V, Bogdanova T, Wienberg J, Zitzelsberger H, Unger K. Gain of chromosome band 7q11 in papillary thyroid carcinomas of young patients is associated with exposure to low-dose irradiation. *Proc Natl Acad Sci U S A*. 2011; 108:9595-9600.
 26. Kaiser JC, Meckbach R, Eidemüller M, Selmansberger M, Unger K, Shpak V, Blettner M, Zitzelsberger H, Jacob P. Integration of a radiation biomarker into modeling of thyroid carcinogenesis and post-Chernobyl risk assessment. *Carcinogenesis*. 2016; 37:1152-1160.
 27. Muniz M, Riezman H. Trafficking of glycosylphosphatidylinositol anchored proteins from the endoplasmic reticulum to the cell surface. *J Lipid Res*. 2016; 57:352-360.

(Received January 27, 2019; Revised March 29, 2019; Accepted April 5, 2019)